

Transverse magnetoresistance, Hall mobility and Hall constant of thin Cu films deposited onto cleaved mica: Evidence of weak Anderson localization.

Eva Díaz

Departamento de Física, Facultad de Ciencias Físicas y Matemáticas, Universidad de Chile

Guillermo Herrera

Departamento de Física, Facultad de Ciencias Físicas y Matemáticas, Universidad de Chile

Simón Oyarzún

Departamento de Física, CEDENNA, Universidad de Santiago de Chile, USACH

Raul Munoz (✉ ramunoz.alvarado@gmail.com)

Departamento de Física, Facultad de Ciencias Físicas y Matemáticas, Universidad de Chile

Research Article

Keywords: Anderson localization, magnetoresistance, Hall effect

Posted Date: May 20th, 2021

DOI: <https://doi.org/10.21203/rs.3.rs-514413/v1>

License:  This work is licensed under a Creative Commons Attribution 4.0 International License.

[Read Full License](#)

Transverse magnetoresistance, Hall mobility and Hall constant of thin Cu films deposited onto cleaved mica: Evidence of weak Anderson localization.

Eva Díaz¹, Guillermo Herrera¹, Simón Oyarzún² and Raul C. Munoz^{1*}

¹Departamento de Física, Facultad de Ciencias Físicas y Matemáticas, Universidad de Chile

Blanco Encalada 2008, Casilla 487-3

Santiago 8370449, Chile

²Departamento de Física, CEDENNA, Universidad de Santiago de Chile, USACH,

Av. Ecuador 3493, Santiago 9170124, Chile

*Email: ramunoz.alvarado@gmail.com

Abstract. We report the resistivity of 5 Cu films approximately 65 nm thick, measured between 5 K and 290 K, and the transverse magnetoresistance and Hall effect measured at temperatures $5 \text{ K} < T < 50 \text{ K}$. The mean grain diameters are $D=(8.9, 9.8, 20.2, 31.5, 34.7) \text{ nm}$, respectively.

The magnetoresistance signal is positive in samples where $D > L/2$ (where $L=39 \text{ nm}$ is the electron mean free path in the bulk at room temperature), and negative in samples where $D < L/2$. The sample where $D=20.2 \text{ nm}$ exhibits a negative magnetoresistance at $B < 2 \text{ Tesla}$ and a positive magnetoresistance at $B > 2 \text{ Tesla}$. A negative magnetoresistance in Cu films has been considered evidence of charge transport involving weak Anderson localization. These experiments reveal that *electron scattering by disordered grain boundaries found along L leads to weak Anderson localization*, confirming the localization phenomena predicted by the quantum theory of resistivity of nanometric metallic connectors. *Anderson localization becomes a severe obstacle for the successful development of the circuit miniaturization effort pursued by the electronic industry, for it leads to a steep rise in the resistivity of nanometric metallic connector with decreasing wire dimensions ($D < L/2$) employed in the design of Integrated Circuits.*

(Submitted to Scientific Reports)

Introduction.

In 1965 Gordon Moore—cofounder of INTEL—proposed an empirical relation according to which the number of transistors per unit area doubled approximately every 24 months; this became known as “Moore’s law”. For this relation to hold, the resistivity of the metallic lines that connect the transistors in an IC must remain the same as the linear dimensions shrink. However, in 2016 INTEL announced that “Moore’s law” is coming to a halt because the resistivity of Cu interconnects increases with shrinking dimensions. Although the increase in resistivity with shrinking wire dimensions seems an accepted fact, the reasons why such an increase takes place remain unknown; this has become a major obstacle that must be overcome to warrant the success of the continuing effort of circuit miniaturization. According to the road map provided by the IDRS, interconnects are expected to reach widths on the range of 10 to 20 nm within the next decade [1]. Therefore, elucidating and understanding why such an increase takes place has become a central problem within the electronic industry.

We published the first quantum theory of resistivity of nanometric metallic structures arising from electron scattering by grain boundaries and by rough surfaces [2, 3], that allows an estimation of the resistivity of nanometric metallic wires of rectangular cross section in terms of the reflection coefficient R that describes electron scattering *from a single grain boundary*, and in terms of the statistical parameters that describe both the roughness of the surfaces limiting the wire as well as the positional disorder of the grain boundaries within the wire; these statistical parameters are directly measurable on the metallic specimen. This quantum theory (when applied to Cu wires of rectangular cross section)—employing no adjustable parameters—provides the first explanation for the increase in resistivity of about an order of magnitude with shrinking lateral dimensions measured in these wires at room temperature: *Such increase in resistivity is to be expected, for it arises from size effects* (from electron scattering by the rough surfaces limiting the wires as well as by electron scattering from disordered grain boundaries found along an electron mean free path in the bulk) [4].

A peculiar feature of this quantum theory, is that it predicts that when the mean grain diameter D characterizing the grain size distribution in the nanometric metallic connector is appreciably smaller than $L(T)$, the electron mean free path in the bulk at temperature T , then electron scattering by successive disordered grain boundaries found along a mean free path becomes dominant, and contributes significantly to the increase in resistivity with shrinking wire dimensions, leading to weak

Anderson localization. *A distinctive feature of weak Anderson localization is that it gives rise to a negative transverse magnetoresistance.*

In previous research work we measured the magnetoresistance as well as the Hall voltage and the Hall constant on a family of thin gold films deposited onto cleaved mica substrates [5-9]. Most of this work dealt with the magnetoresistance measured on gold films deposited onto mica substrates where the samples were made out of columnar grains extending from the top to the bottom surface of the film [5-9]; only in Ref. 10 we measured these transport coefficients (magnetoresistance and Hall voltage) in samples made out of both columnar grains as well as samples made out of grains whose typical diameter D was smaller than the film thickness t . The measurement of the Hall voltage in these gold films provides some strong empirical evidence that allows elucidating whether charge transport across the sample is controlled by electron-surface scattering (as indicated by a Hall mobility that increases linearly with film thickness t in samples made out of columnar grains), or by electron-grain boundary scattering (as indicated by a Hall mobility that increases linearly with the grain diameter D making up the samples when $D < t$). The measurement of the Hall effect in gold samples made out of columnar grains, can also be used to measure nondestructively, the thickness t of the sample, by measuring its Hall voltage [7]. Based upon these results we decided to measure the Hall voltage, the transverse magnetoresistance and the Hall constant in thin Cu films deposited onto cleaved mica substrates varying the mean grain diameter D making up the samples. In this paper we report such measurements.

The content of the paper is organized as follows: In Section 2 we describe briefly the experimental method. In Section 3 we present the results regarding the resistivity of the samples measured between 5 K and 300 K, as well as the transverse magnetoresistance, the Hall voltage, the Hall mobility and the Hall constant measured between 5 K and 50 K. In Section 4 we present the theory used to describe the negative magnetoresistance, that has been considered the “fingerprint” of weak electron localization in thin films. In Section 5 we present a discussion of the results.

Experimental.

The experimental set up used to prepare a family of Cu films approximately 65 nm thick evaporated onto cleaved mica substrates employing Cu 99.9999% pure as a starting material, using a UHV evaporation station, has been briefly described in Section 3 of Ref. 4, and is schematically displayed in Figure 2 of Ref. 4. Changing the substrate temperature from -190 °C to some 35 °C, we

were able to control the mean grain diameter D making up the samples from some 9 nm to about 35 nm. Following results published by Zarate et al. [11], the Cu films were covered with a 3 nm thick TiO film at room temperature to passivate the samples before transferring them to a cryostat, in order to perform transport measurements. The mask employed to evaporate the Cu films onto freshly cleaved mica, is displayed in Figure 1.

Transport measurements were performed by the four-probe method using a Mini Cryogen Free system from Cryogenic Ltd. We measured the temperature dependence of the resistivity for the entire set of samples between 5 K and 290 K, as well as the transverse magnetoresistance and the Hall effect between 5 K and 50 K, the results are reported below.

Results.

We prepared a family of 5 Cu films deposited on mica, whose characteristics are displayed in Table 1.

A. Temperature dependence of the resistivity.

The temperature dependence of the resistivity of different samples is displayed in Figure 2, and in the inset the resistivity of the samples measured at 5 K and 290 K is plotted as a function of the average grain size D .

B. Transverse magnetoresistance.

Let us consider a film oriented along the (x, y) plane, with a magnetic field of strength B oriented along z . The magnetoresistance at temperature T is defined as the fractional change in resistivity $\rho(B, T)$ induced by the presence of the magnetic field B

$$\frac{\Delta\rho(B, T)}{\rho(0, T)} = \frac{\rho(B, T) - \rho(0, T)}{\rho(0, T)}$$

where $\rho(B, T)$ is the resistivity measured at temperature T under an applied magnetic field of strength B .

The transverse magnetoresistance of the samples measured at 5 K is displayed in Figure 3, and the magnetoresistance plotted as a function of temperature is displayed in Figure 4.

C. Hall mobility.

Carriers moving under the presence of an electric field \vec{E} and a magnetic field \vec{B} experience a Lorentz force that results in an average velocity

$$\langle \vec{v} \rangle = \mu_D \vec{E} + \mu_D \mu_H \vec{E} \times \vec{B}$$

where μ_D is the drift mobility and μ_H is the Hall mobility. Under an applied electric field $\vec{E} = (E_x, E_y, 0)$ and $\vec{B} = (0, 0, B)$, we have $(\langle v_x \rangle, \langle v_y \rangle, \langle v_z \rangle) = (E_x + \mu_H E_y B, E_y - \mu_H E_x B, 0)$. The Hall field E_H is defined as the transverse field needed to cancel out the transverse component of the drift velocity $\langle v_y \rangle = 0$; it is given by $E_H = \mu_H E_x B$. The Hall tangent is defined by $\tan \theta_H = \frac{E_H}{E_x} = \mu_H B$ and the Hall mobility is defined by $\mu_H = \frac{\partial \tan \theta_H}{\partial B}$

The Hall tangent measured for the entire set of samples at 5 K is displayed in Figure 5, and in the inset the Hall mobility measured at 5 K is plotted as a function of the average grain diameter D . The temperature dependence of the Hall mobility of different samples is displayed in Figure 6.

D. Hall constant.

The Hall constant is defined as

$$R_H = \frac{E_H}{\sigma E_x B} = -\frac{1}{ne} \frac{\mu_H}{\mu_D} = R_0 \frac{\tan \theta_H}{B} = \rho \mu_H = R_0 r$$

where $R_0 = -\frac{1}{ne}$ represents the Hall constant corresponding to the electron gas in Cu; R_H/R_0 is the normalized Hall constant. Here e is the electron charge, n the electron density, and r is the mobility ratio [$r = \mu_H/\mu_D$]. The normalized Hall constant at 5 K plotted as a function of mean grain diameter D is displayed in Figure 7; in the inset we plot the magnetic field dependence of the normalized Hall constant measured at 5K. The temperature dependence of the normalized Hall constant is plotted in Figure 8.

Theory.

The theory of quantum corrections to the conductivity arising from the spin orbit interaction in a two-dimensional system containing a random potential leading to a negative magnetoresistance was developed in the early eighties [12, 13]. The theory has been applied to explain the negative magnetoresistance in thin Cu films reported by several authors [14-18].

The basic result is that obtained by Hikami, Larkin and Nagaoka (HLN) [12], where in absence of magnetic impurities and under a weak spin-orbit interaction, the magneto-conductivity $\Delta\sigma_{\perp}$ is [eq. (18) in Ref. 12]

$$\Delta\sigma_{\perp} = -\frac{\alpha e^2}{2\pi^2\hbar} \left[\ln\left(\frac{B\phi}{B}\right) - \psi\left(\frac{1}{2} + \frac{B\phi}{B}\right) \right] \quad (1)$$

Here B is the applied magnetic field, e the elementary electron charge, α a scaling factor and ψ the digamma function. The characteristic magnetic field B_{ϕ} is defined by $B_{\phi} = \frac{\hbar}{4el_{\phi}^2}$, where l_{ϕ} corresponds to the phase coherence length.

Discussion.

It seems interesting to note that when the mean grain diameter D decreases from 34.7 nm to 8.9 nm, the resistivity at 5 K increases by nearly one order of magnitude, and it increases monotonically with increasing temperature T . The Hall mobility μ_H at 5 K also increases by nearly one order of magnitude with increasing D from 8.9 nm to 34.7 nm, and it decreases with increasing temperature. This is in sharp contrast to the normalized Hall constant R_H/R_0 that exhibits a rather mild dependence both on T and on D , and turns out to be independent of the strength of the magnetic field B .

This sharp distinction between the grain size dependence of the resistivity and Hall mobility on the one hand, and the Hall constant on the other, is reminiscent of the classical theory of mobility developed in crystalline semiconductors characterized by a spherical Fermi surface, employing solutions of the Boltzmann Transport Equation within the relaxation time approximation $\tau(\epsilon)$. The mobility ratio turns out to be $r = \mu_H/\mu_D = \langle\tau(\epsilon)^2\rangle/\langle\tau(\epsilon)\rangle^2$, where the bracket indicates the average of the energy-dependent relaxation time $\tau(\epsilon)$ employing a weighting function involving the equilibrium electron distribution function $f_0(\epsilon)$ [7, 19].

If we were to apply these arguments to a metallic specimen endowed with a spherical Fermi surface (rather than to a semiconductor), since the carriers involved in charge transport are those located on the Fermi sphere, we would arrive at the conclusion that $r = \langle\tau(\epsilon)^2\rangle/\langle\tau(\epsilon)\rangle^2$, hence $r = 1$ and $R_H = R_0$. However, Cu is characterized by a Fermi surface that is not a perfect sphere, but consists instead of a sphere plus some necks that bulge out in the $\langle 1,1,1 \rangle$, $\langle -1,1,1 \rangle$, $\langle 1,-1,1 \rangle$ and $\langle 1,1,-1 \rangle$ directions. The experimental results displayed in Figures 7 and 8 indicate that the normalized Hall constant is roughly independent of B and it exhibits a mild temperature dependence (within the range 1 Tesla $< B < 5$ Tesla, 5 K $< T < 50$ K), despite the fact that the charge transport process involves

several microscopic electron scattering mechanisms (some of which are temperature-dependent) that are characterized by quite different strengths on the different samples; this point will be revisited below.

However, the most interesting and intriguing result of measuring these magneto transport coefficients, is the remarkable change of sign of the magnetoresistance measured at 5 K displayed in Figure 3, that is positive for the samples made up of grains where the average diameter is $D = 31.5$ nm and 34.7 nm, and is negative on the samples where $D = 8.9$ nm and 9.8 nm. In the sample where $D = 20.2$ nm, there is a mixed behavior, a magnetoresistance that is initially negative at small magnetic fields $B < 2$ T and then becomes positive as the strength of the magnetic field grows larger than 2 T.

A positive magnetoresistance means that the resistivity increases upon the application of a magnetic field B perpendicular to the film. A negative magnetoresistance, however, means that *the resistivity decreases (and hence the conductivity increases) upon applying a magnetic field*. Such increase in conductivity has been considered a signature of (weak) Anderson localization, and arises when the destructive interference between the wave packets representing the charge carriers interacting with several disordered scattering centers is suppressed because the magnetic field induces a phase factor that *reduces the amount of destructive interference* between these two wave packets [one traveling in the forward and the other traveling in the backwards (reverse) order], hence *the conductivity increases* [12]. Reports of weak localization in thin Cu films have already been published [13-18]. Nevertheless, in the films reported in the present work, the negative magnetoresistance is attributed to electron scattering that becomes dominant as the average size D of the grains making up the sample becomes appreciably smaller than the electronic mean free path \square in the bulk, say $D < \square/2$.

We employed the HLN theory to describe the magneto conductivity curves at 5K by fitting equation (1) and using as free parameters the phase coherence length l_ϕ and the scaling factor α . In Figure 9 we display the magneto conductivity curves and the fits as a function of the applied magnetic field in the range from -1 T to 1 T, obtaining l_ϕ for the three samples where weak localization is present. We observe a good agreement between the data and the fits, where the values obtained for l_ϕ are larger than the film thickness, justifying the use of the 2D HLN model.

These experimental results confirm the electron localization phenomena [taking place when $D < L/2$] predicted by the quantum theory of electron transport in nanometric metallic structures. This,

together with the break-down of Moore's law observed with shrinking wire dimensions correctly predicted by theory [4], may be considered as a strong evidence that supports and justifies the description of electron motion upon which the theory of resistivity of nanometric metallic connectors recently published was built. The theory includes a quantum description of each of the following microscopic electron scattering mechanisms that give rise to the observed resistivity: (a) scattering by impurities/point defects, (b) scattering by acoustic phonons, (c) scattering by the rough surfaces limiting the sample and (d) scattering by disordered grain boundaries [2, 3]. The published "fingerprint" of the latter mechanism—of weak Anderson localization arising from electron scattering by disordered grain boundaries—is unambiguously revealed by the experiments reported here, in samples where the average grain diameter D becomes appreciably smaller than the electron mean free path L in the bulk.

The implications for the effort of circuit miniaturization pursued by the electronic industry worldwide are severe, for it turns out that the break-down of Moore's law observed with shrinking wire dimensions—a huge obstacle that stands on the way of successfully continuing the effort of circuit miniaturization—is a natural phenomena correctly predicted by the quantum description of electron transport employing no adjustable parameters [4]. According to the description of electron motion contained in this quantum transport theory, in nanometric metallic connectors where $D < L \ll \lambda$, electron scattering by disordered grain boundaries and electron scattering by the rough surfaces that limit the connector will become dominant and will lead to steep increase in resistivity (of at least an order of magnitude) observed upon shrinking the lateral dimensions of the metallic connector (with decreasing $D < L \ll \lambda$) to a few nm. This is the reason that explains and describes the breakdown of Moore's law.

References.

1. International Road Map for Devices and Systems, 2020 edition.
<https://irds.ieee.org/editions/2020>.
2. Munoz R. C. and Arenas C., Size effects and charge transport in metals: Quantum theory of the resistivity of nanometric metallic structures arising from electron scattering by grain boundaries and by rough surfaces, *Applied Physics Reviews* **4**, 011102 (2017).
3. Arenas C., Henriquez R., Moraga L., Muñoz E. and Munoz R. C., The effect of electron

- scattering from disordered grain boundaries on the resistivity of metallic nanostructures, *Applied Surface Science* **329**, 184 (2015).
4. Arenas C., Herrera G., Munoz E. and Munoz R. C., The breakdown of Moore's law induced by weak Anderson localization and by size effects in nano-scale metallic connectors, *Materials Research Express* **8**, 015026 (2021).
 5. Oyarzun S. et al, Transverse magnetoresistance induced by electron-surface scattering in thin gold films: Experiment and theory, *Applied Surface Science* **289**, 167 (2014).
 6. Munoz R. C., et al., Size Effects under a Strong Magnetic Field: Hall Effect Induced by Electron-Surface Scattering on Thin Gold Films Deposited onto Mica Substrates under High Vacuum, *Phys. Rev. Lett.* **96**, 206803 (2006).
 7. Henriquez R. et al., Size effects on the Hall constant in thin gold films, *J. Appl. Phys.* **108**, 123704 (2010).
 8. Munoz R. C., et al., Size effects under a strong magnetic field: transverse magnetoresistance of thin gold films deposited on mica, *J. Phys.: Condens. Matter* **18**, 3401 (2006).
 9. Munoz R. C., et al., Longitudinal magnetoresistance of thin gold films deposited on mica arising from electron-surface scattering, *Phys. Rev.* **B81**, 165408 (2010).
 10. Henriquez R., et al., Size effects in thin gold films: Discrimination between electron-surface and electron-grain boundary scattering by measuring the Hall effect at 4K, *Appl. Phys. Lett.* **102**, 051608 (2013).
 11. Zarate R. A. and Fuenzalida V., Titanium monoxide ultra-thin coatings evaporated onto polycrystalline copper films, *Vacuum* **76**, 13 (2004).
 12. Hikami S., Larkin A. I. and Nagaoka Y., Spin-orbit interaction and magnetoresistance in the two dimensional system, *Prog. Theor. Physics* **63**, 707 (1980), Physical Society of Japan.
 13. G. Bergmann, Weak localization in thin films, *Physics Reports* **107**, 1 (1984).
 14. Van Haesendonck C., Van der dries L. and Bruynseraede Y., Localization and negative magnetoresistance in thin copper films, *Phys. Rev.* **B25**, 5090 (1982).
 15. Van der dries L., Van Haesendonck C., Bruynseraede Y. and Deutscher G., Two-dimensional localization in thin copper films, *Phys. Rev. Lett.* **46** 565 (1981).
 16. Abraham D. and Rosenbaum R., Magnetoresistance of thin copper films, *Phys. Rev.* **B26**, 1413 (1983).

17. Dai J. and Tang J., weak localization and magnetoresistance in island-like thin copper films, *J. Appl. Phys.* **92**, 6047 (2002).
18. Gershenzon M. E., Gubankov B. N. and Zhuravlev Y. E. , Effect of weak localization and of electron-electron interactions in thin copper and silver films, *Zh. Eksp. Teor. Fiz.* **83**, 2348 (1982).
19. R. A. Smith, *Semiconductors*, Cambridge University Press, Cambridge (1961). Chap. V.

Author Contributions. G. H. prepared the first samples having a grain diameter $D < 10$ nm, and together with S. O. performed the exploratory experiments where the negative magnetoresistance was first detected at 5 K. E. D. performed the systematic sample preparation (involving over 10 samples), and carried out the detailed measurement and analysis of the grain size distribution employing an AFM. E. D. performed, with S. O., the measurement of resistivity, magnetoresistance and Hall effect employing the closed cycle cryostat. S. O. wrote the code and the section describing the analysis of the negative magnetoresistance data. R. M. participated in the planning and design of these experiments, and wrote the manuscript together with S. O.; the manuscript was reviewed by G. H. and E. D.

Competing interests. The authors declare no competing interests.

Table 1. Morphological parameters of the Cu films deposited onto mica substrates. t is the film thickness. The histogram describing the grain size distribution of each sample (measured with an AFM), was fitted to a Gaussian distribution having an average grain diameter D and a standard deviation σ_D , using a set of images of over 1000 grains on samples S1, S2, S4 and S5, and a set of images of 655 grains on S3. $R(5)$ is the resistance of the sample measured at 5 K; $R(290)$ is the resistance of the sample measured at 290 K; l_ϕ is the phase coherence length obtained from fits using the HLN model.

Sample	t [nm]	D [nm]	σ_D [nm]	$R(5)$ [Ω]	$R(290)$ [Ω]	l_ϕ [nm]
S1	67.6	8.9	2.6	3.32	4.27	154
S2	65.4	9.8	2.5	2.91	3.79	127
S3	63.2	20.2	5.7	1.82	2.65	109
S4	69.5	31.5	6.6	0.424	1.21	-
S5	65.3	34.7	8.5	0.397	1.17	-

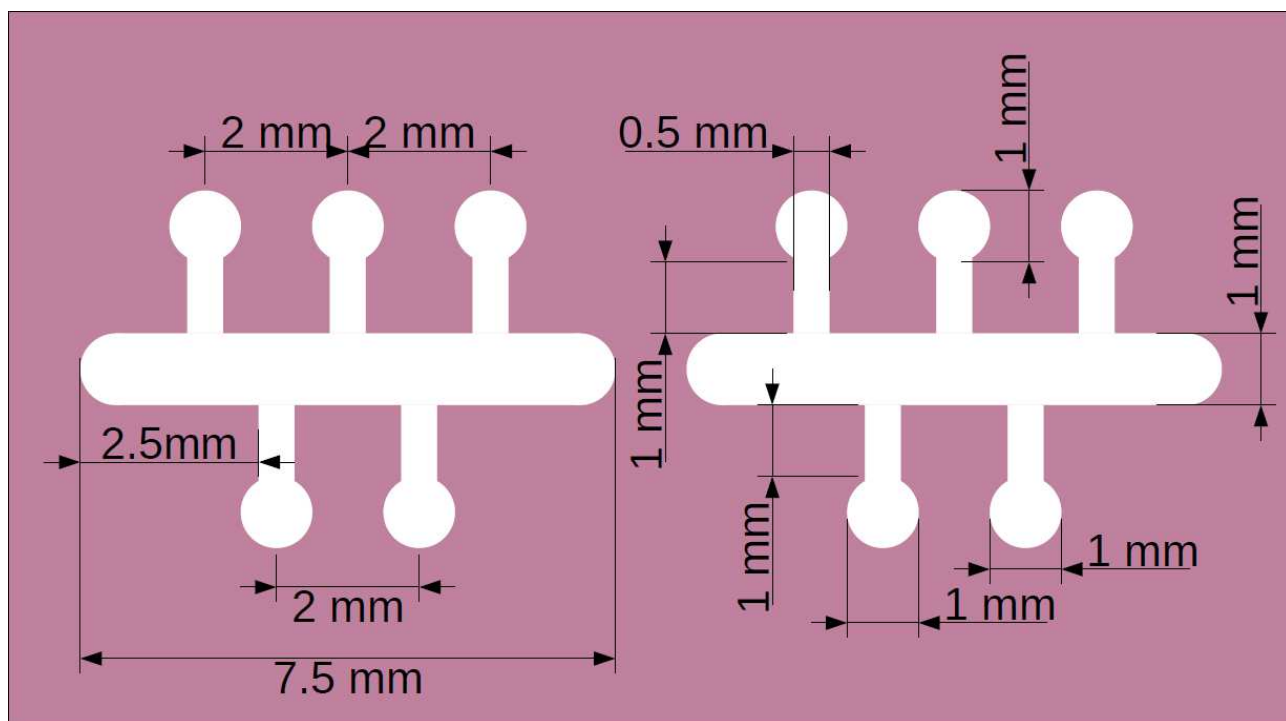


Figure 1. Evaporation mask used to deposit Cu films onto freshly cleaved mica.

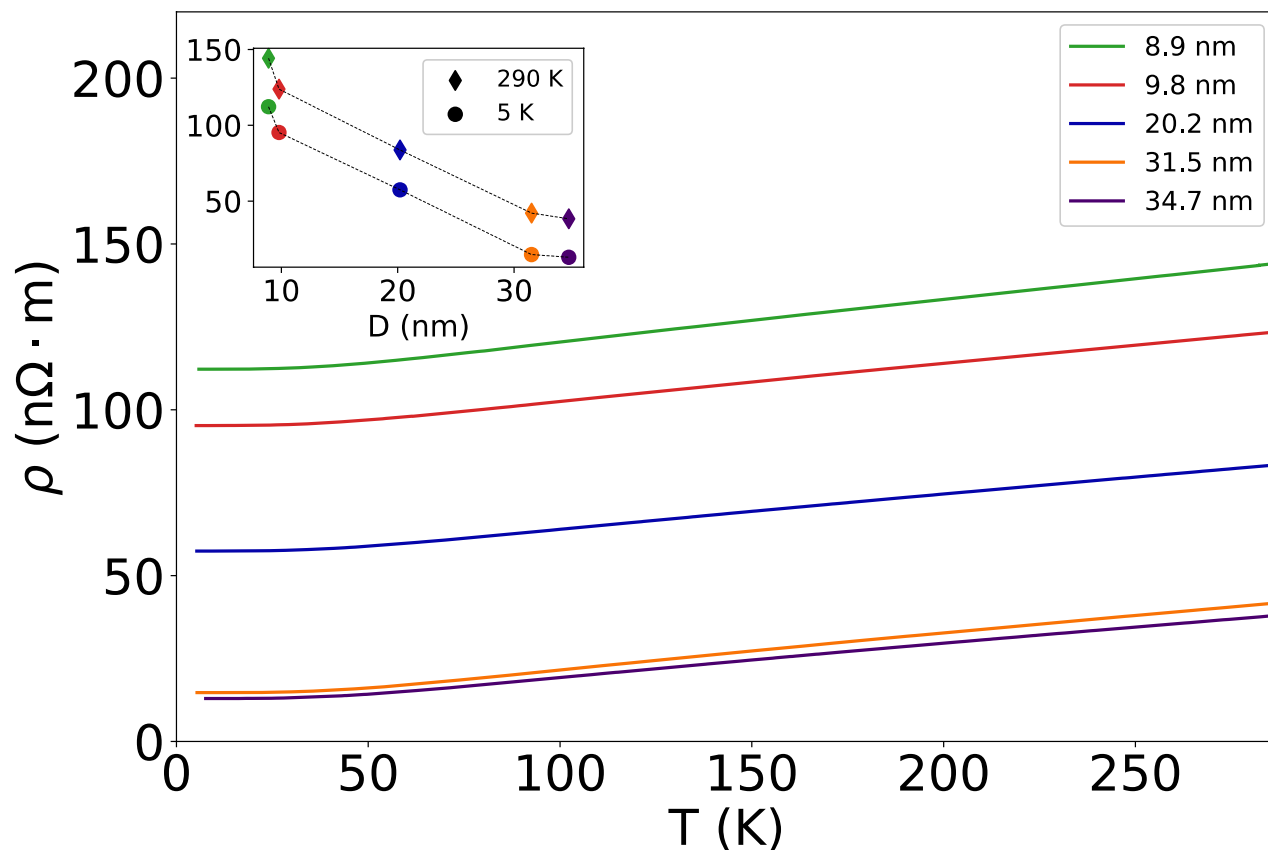


Figure 2. Temperature dependence of the resistivity of the samples measured between 5 K and 290 K. In the inset is displayed the resistivity of the samples measured at 5 K and at 290 K, plotted as a function of the mean grain diameter D .

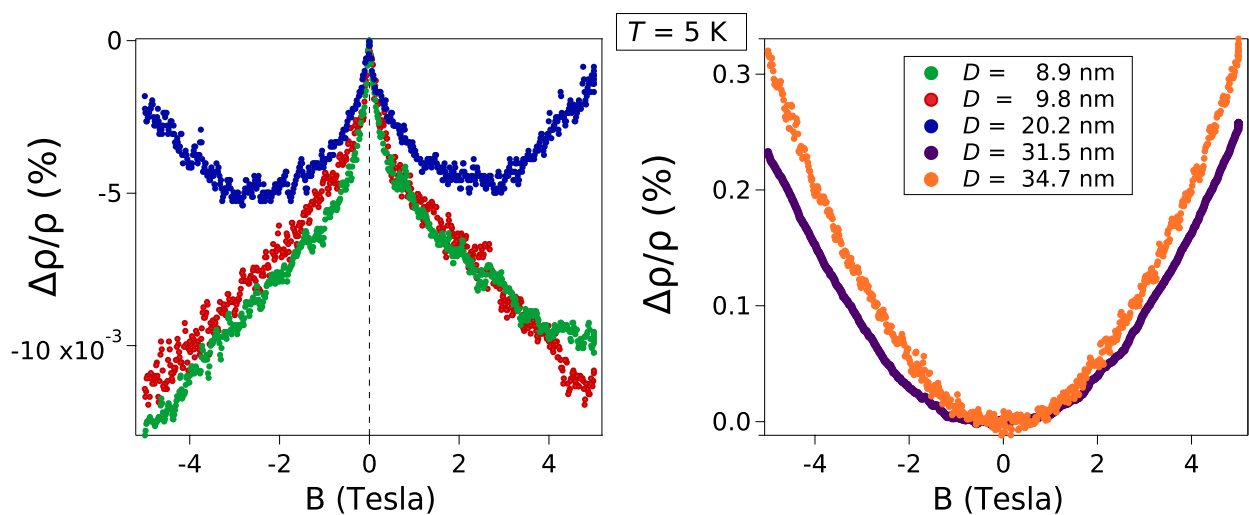


Figure 3. Transverse magnetoresistance of the samples measured at 5 K.

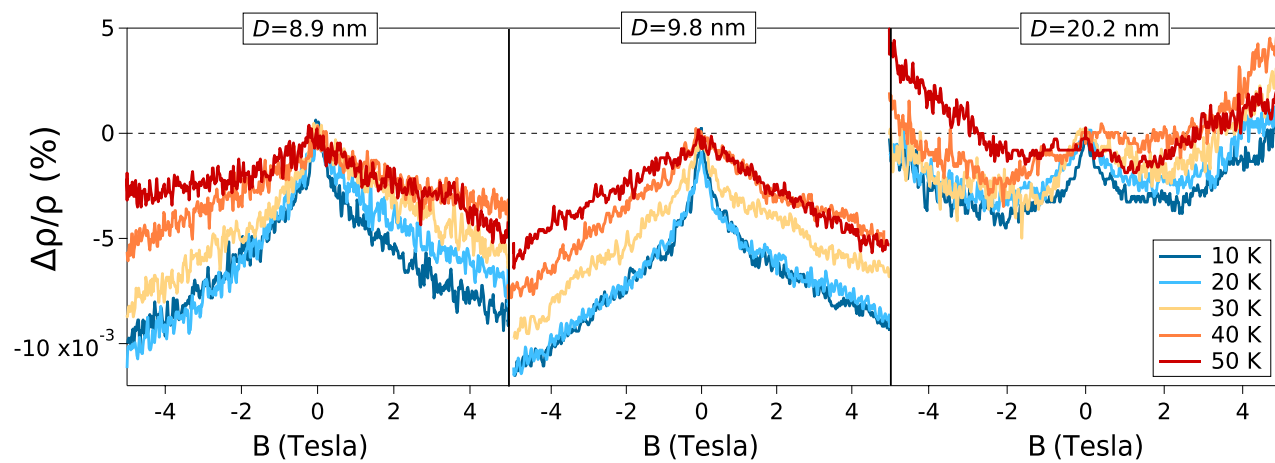


Figure 4. Temperature dependence of the magnetoresistance of the samples for $D = 8.9$ nm, 9.8 nm and 20.2 nm.

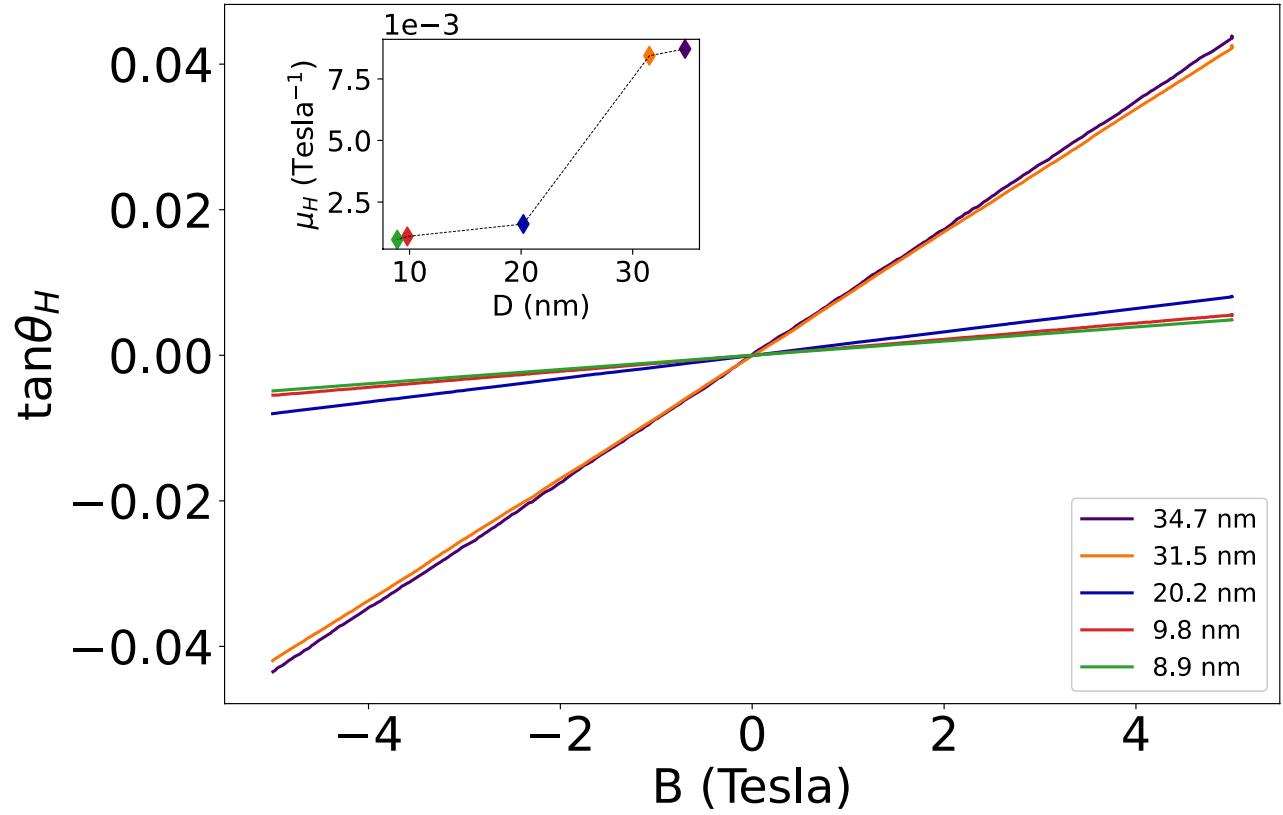


Figure 5. The Hall tangent measured on different samples at 5 K, plotted as a function of magnetic field strength B . In the inset is plotted the Hall mobility measured on different samples at 5K, as a function of the mean grain diameter.

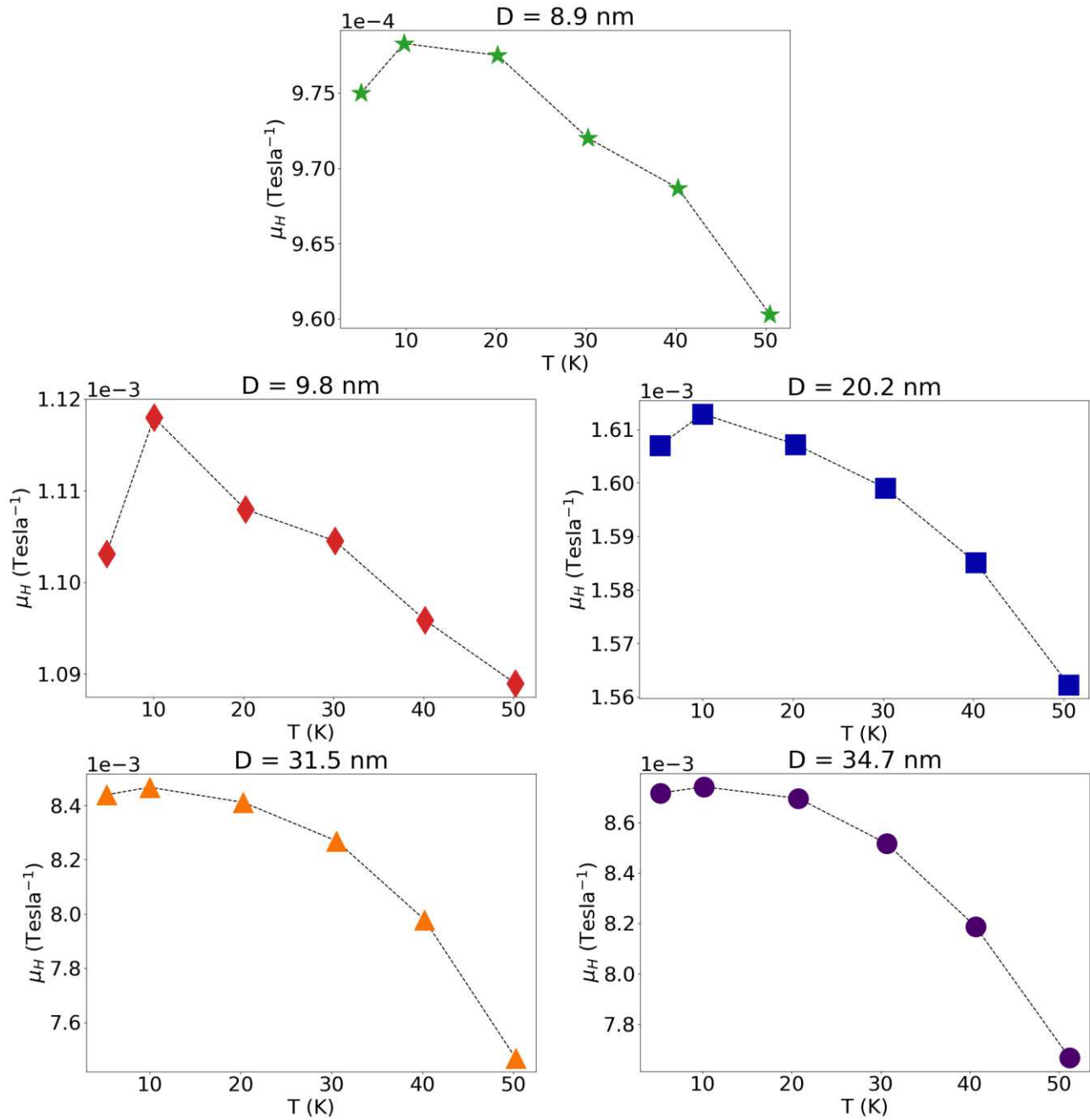


Figure 6. Temperature dependence of the Hall mobility for all samples.

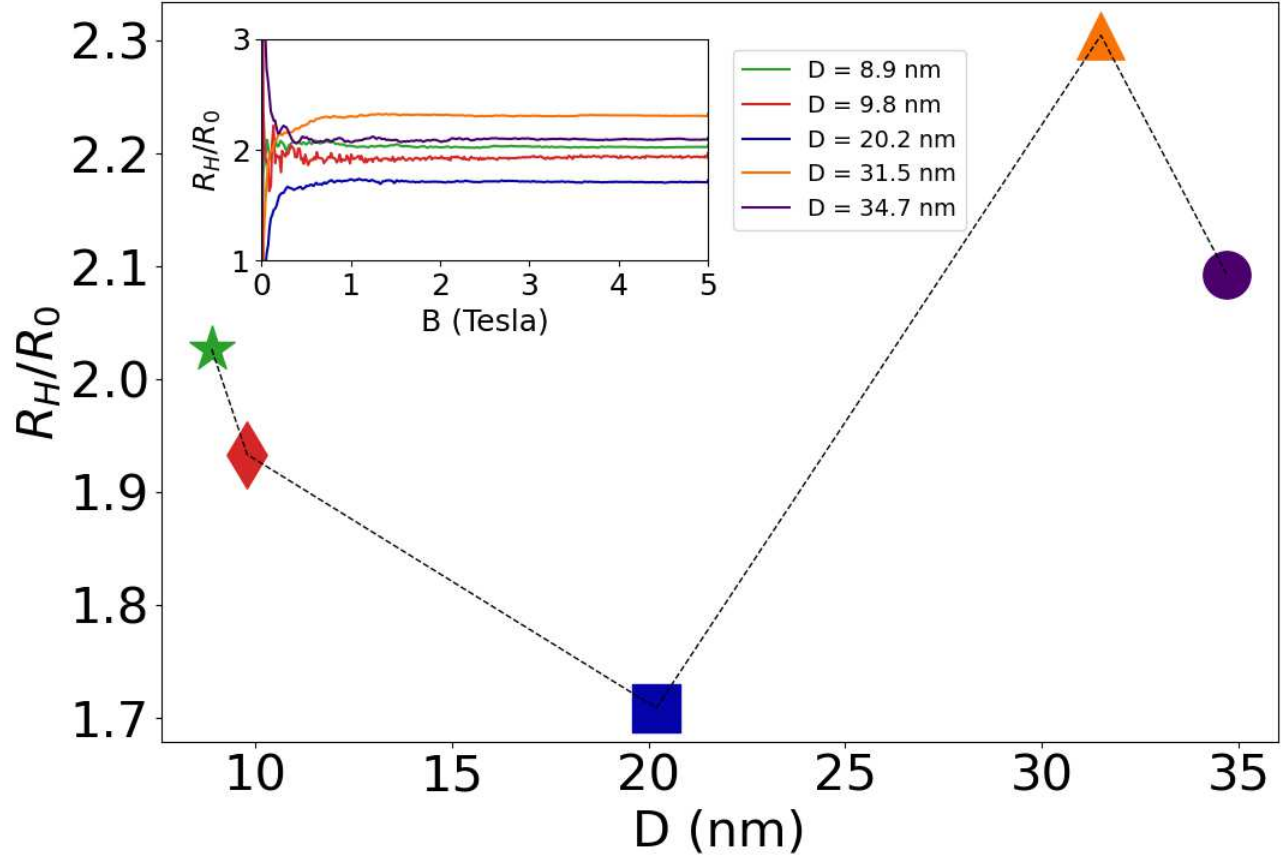


Figure 7. The normalized Hall constant of the samples measured at 5 K plotted as a function of the average grain diameter D , computed from $R_H = \rho\mu_H$. In the inset we plot the magnetic field dependence of the normalized Hall constant measured at 5 K, computed from $R_H = R_0 \frac{\tan \theta_H}{B}$

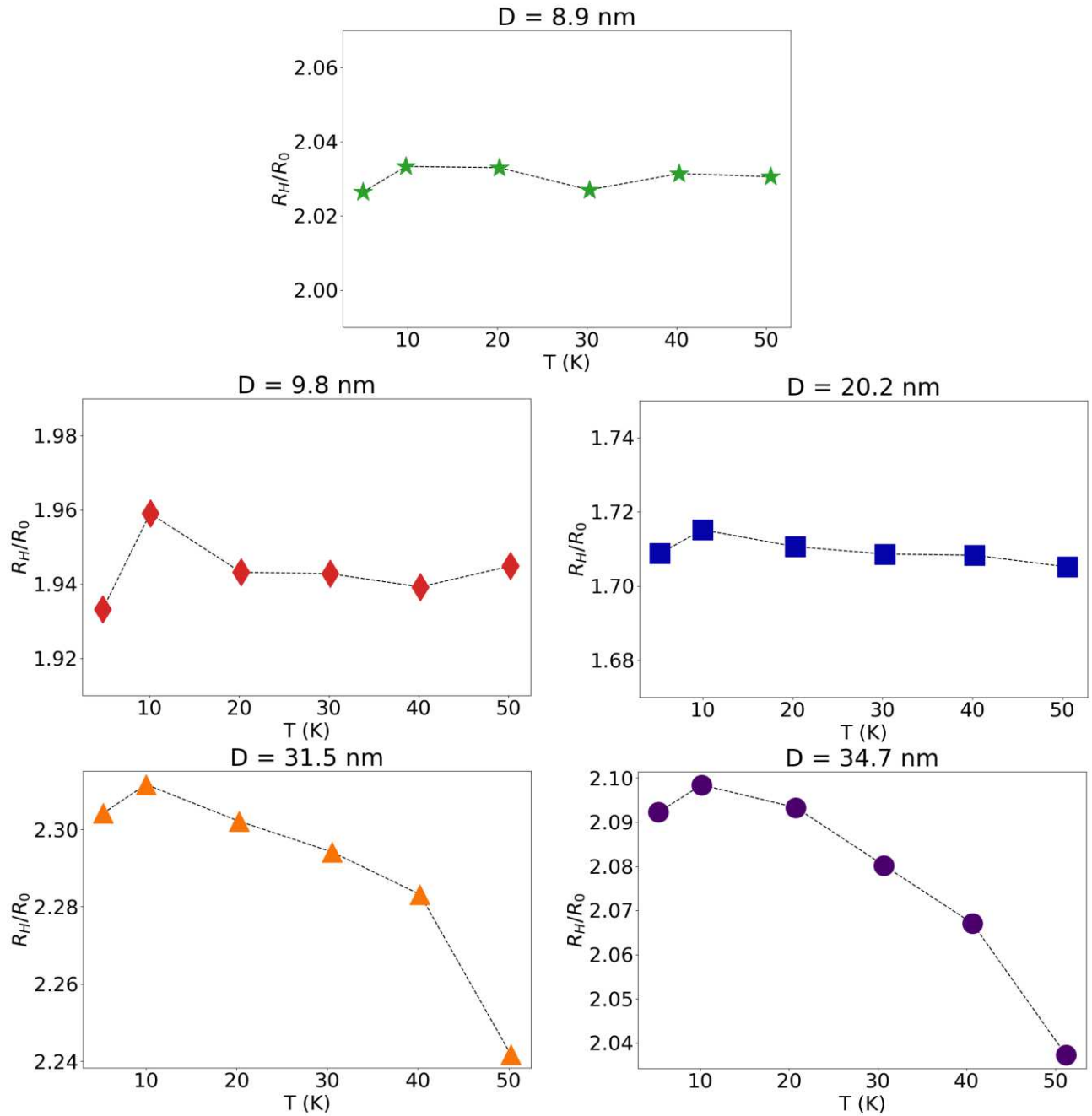


Figure 8. Temperature dependence of the normalized Hall constant for different samples measured at different temperatures, computed from $R_H = \rho\mu_H$.

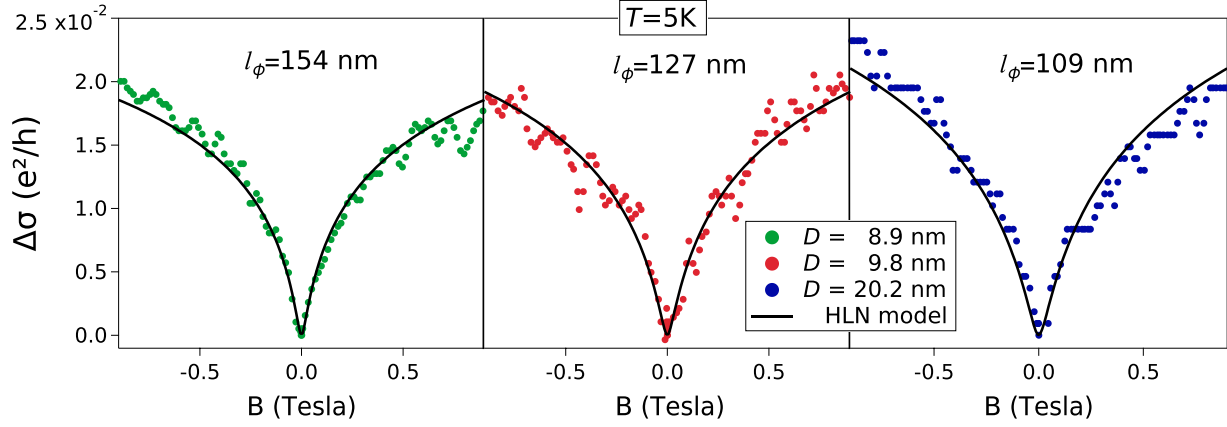


Figure 9. Magnetoconductance curves at 5 K as a function of the applied magnetic field B . The solid lines represent the fitted curves using the HLN model (Ref. 12), equation (1). For the fitted curves we obtained $l_\phi = 154$ nm, 127 nm, 109 nm and $\alpha = -511$, -604 , -747 for the samples S1, S2 and S3, respectively.